

Unexpectedly long-range influence on thin-film magnetization reversal of a ferromagnet by a rectangular array of FeMn pinning films

Yu. P. Kabanov,¹ V. I. Nikitenko,^{1,2} O. A. Tikhomirov,¹ W. F. Egelhoff,² A. J. Shapiro,² and R. D. Shull²

¹*Institute of Solid State Physics, RAS, Chernogolovka 142432, Russia*

²*National Institute of Standards and Technology, Gaithersburg, Maryland 20899, USA*

(Received 25 July 2008; published 30 April 2009)

Exchange bias in bilayer magnetic systems is usually ascribed to the existence of transient magnetic structures at the interfaces between adjacent layers on top of each other. Here, we report the observation of a similar phenomenon in the lateral direction, indicated by an asymmetry in the magnetization reversal of a ferromagnetic film covered with a square grid of an antiferromagnetic layer. We show the antiferromagnet not only changes the properties of the ferromagnet regions immediately underneath it, but despite the large pattern period, also drastically affects the remagnetization behavior in the adjacent uncovered parts of the ferromagnet. Specifically, we demonstrate pattern-controlled nucleation of domain walls and an overall asymmetry in the reversal behavior of the uncovered ferromagnet when the polarity of the in-plane field is reversed. A canted orientation of the intrinsic anisotropy of the ferromagnet with respect to an induced exchange anisotropy and the presence of artificial topologically stable domain walls are discussed as likely origins of the effects.

DOI: 10.1103/PhysRevB.79.144435

PACS number(s): 75.60.Jk, 75.70.Kw, 75.70.Cn

Artificial nanostructures consisting of two or more materials with drastically different magnetic characteristics are the subject of extensive studies in last few decades. The reason for this is the wealth of new magnetic phenomena found and the variety of promising technological applications, including magnetic memory or field sensors using the giant magnetoresistance effect.^{1–10} Recent progress in magnetism widely exploits the idea of artificially imposed boundary conditions to provide materials with unusual magnetic structures and properties. For example the proximity of ferromagnetic (FM) and antiferromagnetic (AFM) layers of a certain thickness gives rise to shifted hysteresis loops.^{9–13} One might also think one could break up the continuous exchange-induced correlation between spins in adjacent grains or islands by the nanoscopic patterning of magnetic films. In this latter case, the magnetostatic interaction predominates the exchange interaction.

The physical origin of the exchange-bias phenomena is the effective fastening of the surface ferromagnetic spins to the adjacent antiferromagnetic material; this fastening is usually hard to switch with a low magnetic field.¹⁰ Close proximity between the spins is necessary for such a mechanism, so the induced influence is typically normal to the layers. As a result, a transient helicoidal spin structure, known as a “partial” (incomplete) heterophase domain wall, or “exchange spring,” is formed. This exchange spring separates the free ferromagnetic spins on one side which are following the external field and the spins on the other side which are pinned to the AF or hard FM layer.^{14–22} For many years this “spring” was considered to be one-dimensional following the pioneering work of Mauri¹⁴ and the magnetization of the whole FM layer was treated as homogeneous due to an assumed soft magnetic character (e.g., low coercivity and anisotropy), as is found when isolated.

Meanwhile, numerous experimental studies of exchange-bias bilayers have shown the importance of the FM domain structure.^{23–36} Moreover, it has been revealed that the elementary events of magnetization reversal possess an un-

expected asymmetry with respect to the applied field sign.^{37–49} It has also been shown by direct experimental studies that the magnetization in the soft FM layer can reverse via the formation of an exchange spring, consisting of subdomains with opposite spin twisting (chirality).^{50–55} Thus the FM layer should not be considered as a passive entity; external in-plane torques from the exchange spring running normal to the layers competes with the in-plane magnetic interactions intrinsic to the FM. Such competition is expected to be especially important in artificially patterned objects developed for up-to-date technological applications.

In the present paper we examine this latter situation by visualizing the kinetics of the magnetization reversal in an artificially constructed sample consisting of a soft ferromagnetic film with a rectangular mesh of antiferromagnetic stripes grown on top of it. We show that despite the relatively large pattern period (100 μm) the antiferromagnet not only changes the properties of the FM regions immediately underneath it, but the AF also affects the magnetization reversal in the adjacent uncovered parts of the ferromagnet. As shown below, pattern-controlled nucleation of domain walls and an overall asymmetry in the reversal behavior of the FM when the polarity of the in-plane field is reversed are two of the most pronounced examples of the lateral influence of the thin AF stripes on the properties of the adjacent FM.

The material under study is based on a 30 nm thick ferromagnetic $\text{Ni}_{77}\text{Fe}_{14}\text{Mo}_5\text{Cu}_4$ film deposited by magnetron sputtering onto a Si(100) wafer having a 250 nm thermal oxide on top. The initial wafers were cleaved into pieces, cleaned ultrasonically in a glassware cleaning solution, rinsed in distilled water, blown dry with inert gas, and installed in the deposition chamber. After bakeout, the deposition chamber had a base pressure of 7×10^{-8} Pa; 90% of the residual is H_2 . The films were deposited at room temperature by dc-magnetron sputtering in a static pressure of 0.3 Pa Ar at a typical rate of ≈ 1 nm/min. After deposition of the FM a saturating magnetic field was applied in the plane of the film, and an additional rectangular mesh of antiferromagnetic

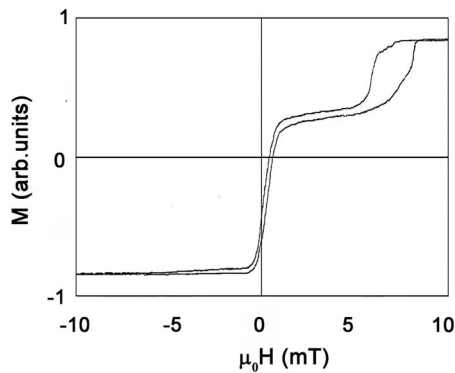


FIG. 1. Macroscopic hysteresis loop of a patterned NiFeMoCu/FeMn bilayer. The curve is obtained at room temperature using a vibrating sample magnetometer. The magnetic field is oriented along the axis of exchange anisotropy induced by the antiferromagnet pattern and the fabrication field.

FeMn was deposited on top. The direction of the magnetic field, marking the axis of the induced exchange anisotropy, coincided with a horizontal side of the pattern in all the following images. In addition, the field used during our magnetization reversal experiments was also applied along the same axis. The spatial period of the AF mesh is $100\ \mu\text{m}$, the width of the stripes is $10\ \mu\text{m}$, and the AF thickness is $10\ \text{nm}$.

The room-temperature macroscopic properties of a resulting patterned structure are described by the hysteresis loop measured in a vibrating sample magnetometer shown in Fig. 1. The loop is obviously asymmetric, confirming the formation of an exchange bias in our system. The left half of the loop, where the external magnetic field is applied along the exchange-bias field, shows only weak change in magnetization. As will be shown later, domain imaging results show that the narrow central part of the loop corresponds to the reversal of bare regions of the FM. For fields in the opposite direction, the pronounced exchange—shifted wide loop at higher fields reflects the magnetization switching of the exchange-biased ferromagnet covered with the AF layer. Note that the central “soft” part of the overall loop is apparently shifted to the right. As from just the magnetization data it is difficult to separate quantitatively the contributions from the covered and bare parts of the ferromagnet, additional spatially resolved measurements are required to determine this correlation. Accordingly, it will be shown that the central soft region is due to the uncovered FM, which has surprisingly experienced some exchange-bias shifting.

Visualization of successive stages of the magnetization reversal was provided using the magneto-optic indicator film (MOIF) technique. The images have been obtained in a polarized light microscope working in the reflection mode. The sample was covered with a probe magneto-optic garnet film sensitive to the perpendicular component of the sample magnetization due to the double Faraday effect. The details on MOIF imaging can be found in Refs. 56–59 and references therein.

A typical MOIF picture of the patterned ferromagnetic/antiferromagnetic sample in the absence of an external magnetic field ($H=0$) is shown in Fig. 2. The vertical and hori-

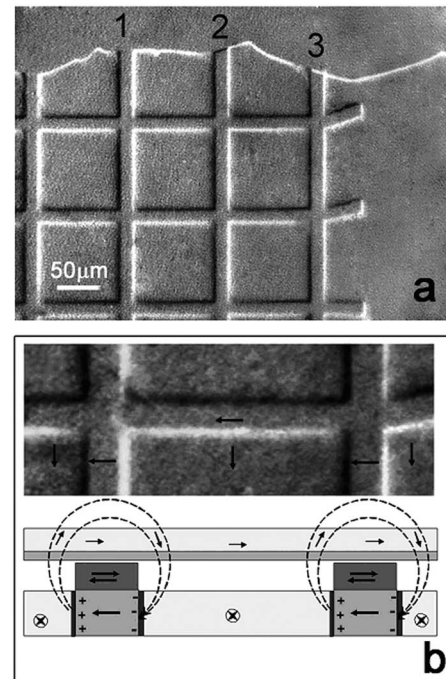


FIG. 2. (a) Typical MOIF image of the patterned FM/AF structure at $\mu_0 H=0$. Bright and dark intensities represent the locations, respectively, of positive and negative stray field sources. The magnetization in both the free part of the ferromagnetic film (right side of the image) and the uncovered parts of the square pattern is approximately vertical; it is an origin of stray field at the horizontal stripes and at the top sample edge. The magnetization direction in those parts of the ferromagnet covered with antiferromagnetic stripes is nearly horizontal (left direction) due to an exchange bias; it creates magneto-optic contrast at the vertical boundaries. (b) map of the magnetization directions in the sample.

zontal stripes correspond to the bilayer regions, i.e., where the FM is covered by the antiferromagnetic FeMn. Hereafter we shall call such bilayer areas the “covered ferromagnet” (CF). The squares between the stripes are the single layer areas of “bare ferromagnet” (BF). Since the majority of the square area of the BF is so far away from the AF, its magnetization is only expected to be affected by the adjacent CF regions via an exchange interaction inside the FM. The right side of Fig. 2(a) also shows the outside part of the FM film not covered with the AF mesh; this part of the sample will be called the “free ferromagnet” and is used as a reference point for comparing the observed magnetization processes.

As usual in MOIF imaging, dark and bright responses of the indicator film show sources of out-of-plane stray fields of opposite sign, while “zero” gray intensity means a homogeneous in-plane magnetization [Fig. 2(b)]. To reconstruct the orientation of magnetization in all parts of the patterned sample, it is necessary to keep in mind that the density of induced magnetic charges is proportional to the relative value of the magnetization component at the boundary between two regions. The strength of the emanated stray field is controlled by the magnetization value of the adjacent ferromagnet, and the typical penetration depth is $\sim 3\ \mu\text{m}$. The outward edge of the sample [zigzag line in the upper part of Fig. 2(a)] is a convenient reference. Note in Fig. 2(a) there is

practically no MOIF response at the intersections of vertical FM/AF stripes with horizontal parts of the sample edge [point 1 in Fig. 2(a)]. However, weak dark and bright responses appear in those places where the edge is, respectively, canted to the left or to the right (points 2 and 3). Such a picture proves the horizontal orientation of the magnetization in the covered FM/AF stripes. This is the same axis along which the saturating field was applied during deposition of the AF. Obviously, the covered ferromagnet is magnetized along the exchange-bias axis formed during the sample preparation (to the left). By comparison, note the MOIF signal is strong and homogeneous along the intersection of the sample edge with parts of the bare and free ferromagnet [Fig. 2(a)]. So we can conclude a big vertical component of the magnetization in these regions. This deduction is confirmed by analysis of the MOIF signal at the boundaries between the covered ferromagnet and the bare one. We see strong stray fields at all these covered/bare boundaries with close values of the MOIF contrast at the vertical and horizontal square sides. Because the covered ferromagnet is magnetized horizontally, this picture is interpreted as indicating a nearly perpendicular orientation of the magnetization in the bare ferromagnet [Fig. 2(b)]. Indeed, the horizontal magnetization in the covered ferromagnet (caused by exchange anisotropy) induces magnetic charges along the vertical square boundaries, while the MOIF signal at the horizontal boundaries is caused by nearly vertical magnetization in the bare ferromagnet. As seen from the MOIF contrast at the sample edge, the absolute value of magnetization in the bare and the free ferromagnet is similar. Therefore it seems reasonable to ascribe the vertical orientation of the magnetization in these parts to a “natural” weak anisotropy of the ferromagnetic film.

We have obtained and studied successive images of the magnetic structure as an in-plane magnetic field was applied along the direction of the induced exchange bias (that is, horizontally to the left in the plane of the subsequent figures). Practically no MOIF contrast is observed inside the whole sample when a high field is applied (image not shown). In this situation the magnetization vectors in all three parts (bare, covered and free ferromagnet) lie close to the field direction, so there are no magnetization discontinuities and no sources of stray field for imaging. When the field value is decreased, the MOIF signal at the edges of the AF stripes appears and intensifies according to a gradual rotation of the magnetization vector in the bare and free parts from the direction of the field to the “natural” anisotropy axis of the FM layer. This stage corresponds to the initial part of the large whole magnetization increase with decreasing field observed on the left side of the hysteresis loop (Fig. 1). At zero field, the magnetization vectors in the covered and bare ferromagnet form the close-to-90° configuration shown in Fig. 2. It is also remarkable that both the bare and free ferromagnetic areas are magnetized homogeneously, so the remnant state of both parts is the same. Furthermore, up to now the MOIF images only showed a rotation of the magnetization in the bare and free ferromagnet, with no domain walls appearing.

When we start to apply and increase the field in the opposite direction, the nucleation and spreading of domains is

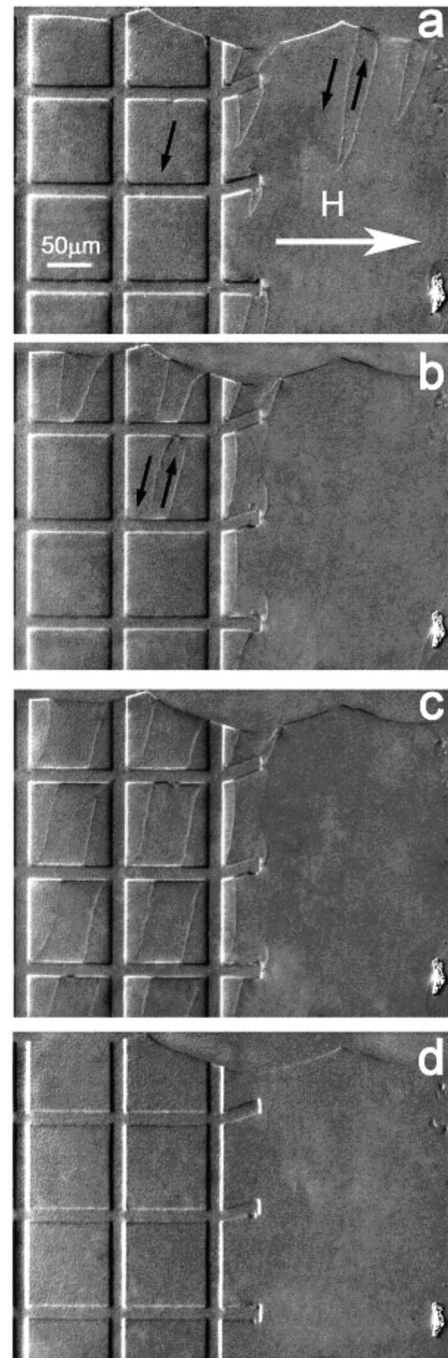


FIG. 3. Evolution of the MOIF image during magnetization reversal. (a) $\mu_0 H = 1.26$ mT, nucleation of wedge domains in the free ferromagnet; (b) $\mu_0 H = 1.32$ mT, nucleation of domains in the bare ferromagnet; (c) $\mu_0 H = 1.38$ mT, lateral spreading of domains in the bare ferromagnet; (d) $\mu_0 H = 6$ mT, antiparallel orientation between the covered and bare ferromagnet. The black arrows indicate the deduced magnetization directions in those regions.

observed first in a lateral part of the sample not covered with the antiferromagnetic pattern [i.e., the free ferromagnet in Fig. 3(a)]. However, we can easily see that there are still no domains in the squares inside the pattern (i.e., in the bare ferromagnet). This is direct evidence that the pattern creates some effect not only on the ferromagnetic film immediately

below the antiferromagnetic layer, but also on retarding the nucleation of domains inside the pattern. Only after the area outside the pattern is completely remagnetized, do domains start to appear in the inner bare area [Fig. 3(b)]. Two features should be noted at this stage. First, there is a clear correlation of the nucleation sites with the AF stripes. Even for the film with such a large $100\ \mu\text{m}$ period macroscopic pattern, the kinetics of the magnetization reversal of the ferromagnetic film is influenced by the antiferromagnetic mesh. The likely reason for this phenomenon is the presence of artificial immobile 90° domain boundaries at the edge of the AF stripes working as nucleation sites for 180° domain walls inside the bare parts. Second, the domain walls in the bare ferromagnet are not vertical but inclined a little bit with respect to the vertical axis. Normally FM domain walls tend to lie parallel to the anisotropy axis in order to avoid additional magnetic charges caused by head-to-head spin configurations. We can therefore conclude that the anisotropy axis of the free part of the ferromagnetic film is oriented at the small angle to the vertical direction.

Motion of the domain walls in the bare ferromagnet can be easily traced by abrupt changes in the stray field sign in those places where the domain wall intersects with a horizontal edge of the sample or antiferromagnetic stripe [Figs. 3(b) and 3(c)]. There is no change in the stray field sign at vertical edges of the pattern because the MOIF signal at the vertical edges is created by the horizontal magnetization of the covered ferromagnet, where the reversal process has not started yet; the field is still too weak to induce any significant rotation of the magnetization in the covered parts which are pinned by a strong exchange anisotropy.

When all domain rearrangements in the bare and free ferromagnet have completed, further increase in the field results in a decrease in the MOIF signal at the horizontal edges. However, the stray field at the vertical edges remains and even becomes stronger [Fig. 3(d)]. Such magneto-optic contrast is expected when there is antiparallel orientation of the spins in the bare and covered regions. Indeed, the hysteresis loop in Fig. 1 shows the picture in Fig. 3(d) corresponds to the situation where the magnetization in the soft bare ferromagnet is saturated in the direction of the field (that is, to the right), while the spins in the covered part have not yet changed from their opposite exchange-bias direction. It can also be seen that the width of the areas where the sample stray field is localized is now larger, seeming almost to continue through the horizontal AF stripes. These effects are probably coupled to the nucleation of an inhomogeneous 180° -exchange spring in the covered ferromagnet under the action of the magnetic field which is currently antiparallel to the direction of exchange bias. At higher positive field the MOIF contrast becomes weaker, and at the end of the half cycle it is nearly homogeneous (not shown). At that point the whole pattern is now magnetized along the field (to the right).

Backward switching to the left is shown in Fig. 4 as the positive field is reduced. It starts from the magnetization rotation in the covered parts, which creates an increase in the stray field at the horizontal edges of the pattern. It can be seen at Fig. 4(a) that this rotation is inhomogeneous, and that the single domain spring in the covered ferromagnet breaks

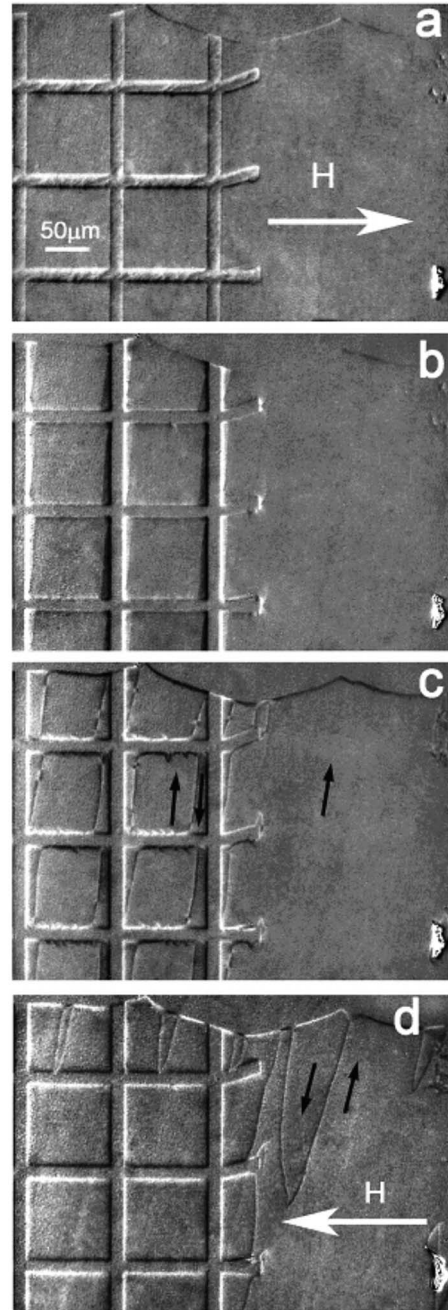


FIG. 4. Evolution of the MOIF image during the backward branch of the magnetization reversal. (a) $\mu_0 H = 7.69$ mT, unfolding of the exchange spring in the covered ferromagnet (note the inhomogeneities and microdomains); (b) $\mu_0 H = 0.06$ mT, diffuse domain walls at the vertical bare/covered ferromagnet boundaries; (c) $\mu_0 H = 0$, the backward branch remnant state—antiparallel domains in the bare ferromagnet; (d) $\mu_0 H = -0.96$ mT, domain processes in the free ferromagnet. The black arrows indicate the deduced magnetization directions in those regions.

into small domains, especially pronounced in the horizontal stripes. This domain-assisted breaking of the uniformity of magnetization in the covered parts occurs in the narrow field interval of a few mT; further decrease in H results in the antiparallel configuration in the covered and bare regions, as shown in Fig. 4(b). At this point the exchange-biased spins in

the covered ferromagnet are strongly enough coupled to the spins in the bare ferromagnet to pull them back from their previous orientations as H is decreased further. Note the stray field areas near the pattern edges are extremely wide and displaced inside the bare ferromagnet squares. Furthermore these transient regions develop into usual ferromagnetic domains [Fig. 4(c)] with subsequent reduction in H . Also, the antiferromagnetic pattern facilitates the nucleation of domains in the bare regions. As a result, the remnant state of the bare ferromagnet in the decreasing positive field branch of the hysteresis loop is different: it contains some domains magnetized up and some magnetized down. Recall that domain nucleation in the covered parts was suppressed during the decreasing-negative magnetization branch of the hysteresis loop [Fig. 3(a)]. For comparison, note there are also no domains in the free ferromagnet [Fig. 4(c)] as in the previous remnant state [Fig. 2(a)]. Domains appear later in the free parts when a field of opposite (i.e., negative) sign is applied to the sample; by that time, domains in the bare ferromagnet have already disappeared [Fig. 4(d)].

With H directed to the left, further increase in its magnitude results in simple rotation of the magnetization vector in the bare and free ferromagnet regions and contains no new features different from the previous approach to saturation for positive (right directed) fields.

The pictures shown above of the magnetization sequences during a field cycle show an obvious asymmetry between the forward and backward branches even in the bare ferromagnet squares not directly covered by the antiferromagnet, but surrounded by adjacent FM/AF stripes along the perimeter. First, nucleation of new domains, their spreading and coagulation take place at different field values for the forward and backward branches. Specifically, remnant states corresponding to $H=0$ are found to be different: no domains in the bare ferromagnet are seen in the former case while they are already present in the latter one. This is direct evidence of the influence of the covered regions in the lateral direction even though the covered regions might be as much as $50 \mu\text{m}$ away from the uncovered region being affected. The likely origin of such in-plane asymmetry is shown in Fig. 5. Due to the fact that the anisotropy axis of the ferromagnet is not strictly vertical, the two states of the bare ferromagnet contain small horizontal components of opposite sign. They interact with the surrounding spins of the covered parts magnetostatically: the density of induced magnetic charges in the “head-to-head” configuration is higher than in the “head-to-tail” one. Quantitatively, the density of magnetic charges at the vertical edges is $2\pi M_s(1-\sin\varphi)$ for the left configuration and $2\pi M_s(1+\sin\varphi)$ for the right one, where φ is the deviation angle of the FM anisotropy axis from the vertical direction, and M_s is the spontaneous magnetization. This difference in energy is equivalent to an effective bias field; an estimation from $\mu H = 4\pi M_s \sin\varphi$ (where μ is magnetic permeability) with $\mu \approx 50\,000$, $M_s \approx 8000$ G, and $\varphi = 12^\circ$ gives $H \approx 0.04$ mT (0.4 Oe). Contrary to the “usual” out-of-plane bias caused by short distance exchange forces, the in-plane interaction can affect relatively distant areas (e.g., the $100 \mu\text{m}^2$ in our experiments). A complementary factor is the presence of artificial 90° domain walls at the interfaces between the covered and bare ferromagnet: the nucleation and

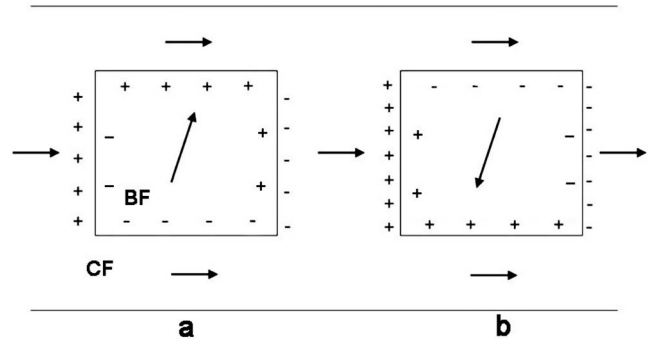


FIG. 5. Two principal configurations of the magnetization for $\mu_0 H = 0$. (a) The correlation between the magnetization directions in the covered and bare ferromagnet decreases the density of effective magnetic charges at the boundary; (b) the anticorrelation of the horizontal component of the magnetization in the bare and covered ferromagnet induces additional magnetic charges. The difference in magnetostatic energy between the two states causes the creation of a finite effective magnetic field in the lateral direction.

spreading behavior of the 180° walls inside the bare ferromagnet is obviously different in the forward and backward hysteresis branches.

Nucleation and growth of new domains in both the free and bare ferromagnet is a result of the interplay between the negative Zeeman energy of the applied field favoring the magnetization reversal, and the positive surface energy of the domain walls which prevents reversal. However, due to the proximity of adjacent covered regions the value of the external applied fields necessary to induce the characteristic changes in the domain patterns for the two types of ferromagnet are different (see Figs. 3 and 4). Magnetic poles at the natural or artificial edges favor nucleation of the domain walls similar to that favored by minimization of the Zeeman energy. A higher density of poles [Fig. 5(b)] means more magnetostatic energy savings result by forming a domain wall. As a result, nucleation in the bare areas surrounded by the antiferromagnet starts at a higher or smaller field compared to that required for the free areas, depending on the sign of the applied field. This difference results in an effective lateral bias effect induced by the covered ferromagnet. Obviously, this contribution is too weak to change the whole mechanism of magnetization reversal in the sample, but it is finite and it can be determined experimentally by means of magneto-optic imaging.

Apart from the quantitative influence of the AF pattern on the magnetization reversal in the bare ferromagnet, as revealed by the in-plane bias shift, one can also observe another effect: the kinetics of the domain structure variation in the bare ferromagnet is also qualitatively different for the two hysteresis loop branches. This latter difference is shown in detail in Fig. 6. For the forward branch, the process starts from the nucleation and spreading of narrow wedge-shaped domains in the middle of the bare ferromagnet squares [Fig. 6(a)]. The resulting 180° walls travel in the lateral direction [Fig. 6(b)] and disappear at the edges of the covered stripes where the perpendicular orientation of the magnetization is supported by a strong out-of-plane exchange bias from the AF [Fig. 6(c)]. This sequence of domain processes is fol-

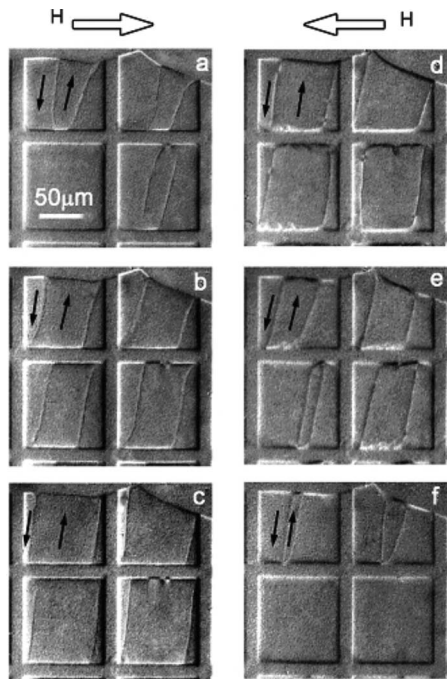


FIG. 6. Asymmetry of the domain structure dynamics during magnetization reversals in opposite directions. Forward branch of the hysteresis loop (nucleation of the wedges in the middle of the squares): (a) $\mu_0 H = 1.32$ mT, (b) $\mu_0 H = 1.38$ mT, (c) $\mu_0 H = 1.62$ mT. Backward branch (nucleation of flat walls at the AF stripes): (d) $\mu_0 H = 0$, (e) $\mu_0 H = -0.84$ mT, (f) $\mu_0 H = -0.88$ mT. The black arrows indicate the deduced magnetization directions in those regions.

lowed by overall rotation of the magnetization in the bare ferromagnet at higher fields. Contrary to this sequence, magnetization reversal in the backward branch is initiated at the

edges of the covered ferromagnet stripes [Fig. 6(d)] where stationary 90° domain walls (not wedges) are generated by artificial boundary conditions. These walls annihilate in the middle of the bare ferromagnet squares [Fig. 6(e)] and finally the residual wedges exit from the sample at its top edge [Fig. 6(f)]. By contrast, for a normal ferromagnet, domains nucleate at the same locations and grow in the same directions for both the forward and reverse branches of its hysteresis loop. These observations confirm that the role of the AF pattern is not simply a consequence of magnetostatic energy considerations, like that shown in Fig. 5. Instead, in the backward branch the AF acts as an artificial nucleation center for the antiparallel domain walls in the bare ferromagnet. This subject will be examined in detail in a future publication.

In conclusion, we have visualized successive stages of the magnetization reversal in a composite system consisting of a soft ferromagnetic film with a square mesh of an antiferromagnet on top of it. Though the magnetization reversals of the covered and bare parts of the sample proceed separately, we have demonstrated definitively the influence of such artificially created boundary conditions on the domain structure dynamics in the ferromagnetic film. First, the remnant state of the ferromagnetic layer becomes qualitatively different for the forward and backward branches of the hysteresis loop if the FM is surrounded along the perimeter by the exchange-biased material. Further, the antiferromagnetic mesh becomes a preferable site for domain nucleation. The patterned structure facilitates nucleation of the oppositely directed domains for one direction of the field, and retards their appearance for the opposite direction of H . The likely reason for the observed asymmetry is the magnetostatic interaction between the covered and bare ferromagnet when there is a canted orientation of their anisotropy axis to that of the AF mesh. Finally, nucleation of new domains in a bare ferromagnet occurs at different sites for the forward and backward magnetization reversals.

- ¹P. Grünberg, R. Schreiber, Y. Pang, M. B. Brodsky, and H. Sowers, *Phys. Rev. Lett.* **57**, 2442 (1986).
- ²M. N. Baibich, J. M. Broto, A. Fert, F. Nguyen Van Dau, F. Petroff, P. Etienne, G. Creuzet, A. Friederich, and J. Chazelas, *Phys. Rev. Lett.* **61**, 2472 (1988).
- ³G. Binasch, P. Grünberg, F. Saurenbach, and W. Zinn, *Phys. Rev. B* **39**, 4828 (1989).
- ⁴S. S. P. Parkin, N. More, and K. P. Roche, *Phys. Rev. Lett.* **64**, 2304 (1990).
- ⁵J. Unguris, R. J. Celotta, and D. T. Pierce, *Phys. Rev. Lett.* **67**, 140 (1991).
- ⁶B. Dieny, V. S. Speriosu, S. S. P. Parkin, B. A. Gurney, D. R. Wilhoit, and D. Mauri, *Phys. Rev. B* **43**, 1297 (1991).
- ⁷J. C. Slonczewski, *J. Magn. Magn. Mater.* **159**, L1 (1996).
- ⁸C. H. Marrows, *Adv. Phys.* **54**, 585 (2005).
- ⁹W. H. Meiklejohn and C. P. Bean, *Phys. Rev.* **102**, 1413 (1956).
- ¹⁰W. H. Meiklejohn and C. P. Bean, *Phys. Rev.* **105**, 904 (1957).
- ¹¹J. Nogues and I. K. Schuller, *J. Magn. Magn. Mater.* **192**, 203 (1999).
- ¹²R. L. Stamps, *J. Phys. D* **33**, R247 (2000).
- ¹³F. Radu and H. Zabel, *Springer Tracts Mod. Phys.* **227**, 97 (2008).
- ¹⁴D. Mauri, H. C. Siegmann, P. S. Bagus, and E. Kay, *J. Appl. Phys.* **62**, 3047 (1987).
- ¹⁵F. Y. Yang and C. L. Chien, *Phys. Rev. Lett.* **85**, 2597 (2000).
- ¹⁶V. I. Nikitenko, V. S. Gornakov, Yu. P. Kabanov, A. J. Shapiro, R. D. Shull, C. L. Chien, J. S. Jiang, and S. D. Bader, *J. Magn. Magn. Mater.* **258-259**, 19 (2003).
- ¹⁷A. Scholl, M. Liberati, E. Arenholz, H. Ohldag, and J. Stöhr, *Phys. Rev. Lett.* **92**, 247201 (2004).
- ¹⁸E. F. Kneller and R. Hawig, *IEEE Trans. Magn.* **27**, 3588 (1991).
- ¹⁹J. S. Jiang, E. E. Fullerton, C. H. Sowers, A. Inomata, S. D. Bader, A. J. Shapiro, R. D. Shull, V. S. Gornakov, and V. I. Nikitenko, *IEEE Trans. Magn.* **35**, 3229 (1999).
- ²⁰K. V. O'Donovan, J. A. Borchers, C. F. Majkrzak, O. Hellwig, and E. E. Fullerton, *Phys. Rev. Lett.* **88**, 067201 (2002).
- ²¹R. Röhlberger, H. Thomas, K. Schlage, E. Burkel, O. Leupold, and R. Ruffer, *Phys. Rev. Lett.* **89**, 237201 (2002).
- ²²V. S. Gornakov, V. I. Nikitenko, A. J. Shapiro, R. D. Shull, J. S.

- Jiang, and S. D. Bader, *J. Magn. Magn. Mater.* **246**, 80 (2002).
- ²³A. A. Glazer, A. P. Potapov, R. I. Tagirov, and Ya. S. Shur, *Sov. Phys. Solid State* **8**, 2413 (1967).
- ²⁴M. Takahashi, A. Yanai, S. Taguchi, and T. Suzuki, *Jpn. J. Appl. Phys. Part 1* **19**, 1093 (1980).
- ²⁵J. Zhu, Y. Zheng, and X. Lin, *J. Appl. Phys.* **81**, 4336 (1997).
- ²⁶V. I. Nikitenko, V. S. Gornakov, L. M. Dedukh, Yu. P. Kabanov, A. F. Khapikov, A. J. Shapiro, R. D. Shull, A. Chaiken, and R. P. Michel, *J. Appl. Phys.* **83**, 6828 (1998).
- ²⁷M. D. Stiles and R. D. McMichael, *Phys. Rev. B* **59**, 3722 (1999).
- ²⁸H. D. Chopra, D. X. Yang, P. J. Chen, H. J. Brown, L. J. Swartzendruber, and W. F. Egelhoff, *Phys. Rev. B* **61**, 15312 (2000).
- ²⁹J. Yu, A. D. Kent, and S. S. S. Parkin, *J. Appl. Phys.* **87**, 5049 (2000).
- ³⁰Z. Li and S. Zhang, *Phys. Rev. B* **61**, R14897 (2000).
- ³¹M. Cartier, S. Auffert, Y. Samson, P. Bayle-Guillemaud, and B. Dieny, *J. Magn. Magn. Mater.* **223**, 63 (2001).
- ³²J. P. King, J. N. Chapman, M. F. Gillies, and J. S. C. Kools, *J. Phys. D* **34**, 528 (2001).
- ³³A. Kirilyuk, Th. Rasing, H. Jaffres, D. Lacour, and F. N. Van Dau, *J. Appl. Phys.* **91**, 7745 (2002).
- ³⁴F. Offi, W. Kuch, L. I. Chelaru, M. Kotsugi, and J. Kirschner, *J. Magn. Magn. Mater.* **261**, L1 (2003).
- ³⁵C. L. Chien, V. S. Gornakov, V. I. Nikitenko, A. J. Shapiro, and R. D. Shull, *Phys. Rev. B* **68**, 014418 (2003).
- ³⁶S. Mangin, T. Hauet, Y. Henry, F. Montaigne, and E. E. Fullerton, *Phys. Rev. B* **74**, 024414 (2006).
- ³⁷V. I. Nikitenko, V. S. Gornakov, L. M. Dedukh, Yu. P. Kabanov, A. F. Khapikov, A. J. Shapiro, R. D. Shull, A. Chaiken, and R. P. Michel, *Phys. Rev. B* **57**, R8111 (1998).
- ³⁸V. I. Nikitenko, V. S. Gornakov, L. M. Dedukh, A. F. Khapikov, A. J. Shapiro, R. D. Shull, and A. Chaiken, *J. Magn. Magn. Mater.* **198-199**, 500 (1999).
- ³⁹V. I. Nikitenko, V. S. Gornakov, A. J. Shapiro, R. D. Shull, K. Liu, S. M. Zhou, and C. L. Chien, *Phys. Rev. Lett.* **84**, 765 (2000).
- ⁴⁰K. Liu, S. M. Zhou, C. L. Chien, V. I. Nikitenko, V. S. Gornakov, A. J. Shapiro, and R. D. Shull, *J. Appl. Phys.* **87**, 5052 (2000).
- ⁴¹M. R. Fitzsimmons, P. Yashar, C. Leighton, I. K. Schuller, J. Nogues, C. F. Majkrzak, and J. A. Dura, *Phys. Rev. Lett.* **84**, 3986 (2000).
- ⁴²Z. Li and S. Zhang, *Appl. Phys. Lett.* **77**, 423 (2000).
- ⁴³M. Gierlings, M. J. Prandolini, H. Fritzsche, M. Gruyters, and D. Riegel, *Phys. Rev. B* **65**, 092407 (2002).
- ⁴⁴Y. G. Wang and A. K. Petford-Long, *J. Appl. Phys.* **92**, 6699 (2002).
- ⁴⁵V. K. Vlasko-Vlasov, U. Welp, Z. J. Guo, J. S. Jiang, J. E. Pearson, J. P. Liu, D. J. Miller, Y. Tang, and S. D. Bader, *J. Appl. Phys.* **93**, 6486 (2003).
- ⁴⁶B. Beckmann, U. Nowak, and K. D. Usadel, *Phys. Rev. Lett.* **91**, 187201 (2003).
- ⁴⁷P. Blomqvist, K. M. Krishnan, and H. Ohldag, *Phys. Rev. Lett.* **94**, 107203 (2005).
- ⁴⁸J. Camarero, J. Sort, A. Hoffmann, J. M. Garcia-Martin, B. Dieny, R. Miranda, and J. Nogues, *Phys. Rev. Lett.* **95**, 057204 (2005).
- ⁴⁹Z. P. Li, O. Petravic, R. Morales, J. Olamit, X. Batlle, K. Liu, and I. K. Schuller, *Phys. Rev. Lett.* **96**, 217205 (2006).
- ⁵⁰R. D. Shull, A. J. Shapiro, V. S. Gornakov, V. I. Nikitenko, J. S. Jiang, H. Kaper, G. Leaf, and S. D. Bader, *IEEE Trans. Magn.* **37**, 2576 (2001).
- ⁵¹J. S. Jiang, S. D. Bader, H. Kaper, G. K. Leaf, R. D. Shull, A. J. Shapiro, V. S. Gornakov, V. I. Nikitenko, C. L. Platt, A. E. Berkowitz, S. David, and E. E. Fullerton, *J. Phys. D* **35**, 2339 (2002).
- ⁵²Yu. P. Kabanov, V. S. Gornakov, V. I. Nikitenko, A. J. Shapiro, and R. D. Shull, *J. Appl. Phys.* **93**, 8244 (2003).
- ⁵³V. S. Gornakov, Yu. P. Kabanov, V. I. Nikitenko, O. A. Tikhomirov, A. J. Shapiro, and R. D. Shull, *J. Exp. Theor. Phys.* **99**, 602 (2004).
- ⁵⁴Y. Henry, S. Mangin, F. Montaigne, *Phys. Rev. B* **69**, 140401(R) (2004).
- ⁵⁵V. S. Gornakov, Yu. P. Kabanov, O. A. Tikhomirov, V. I. Nikitenko, S. V. Urazhdin, F. Y. Yang, C. L. Chien, A. J. Shapiro, and R. D. Shull, *Phys. Rev. B* **73**, 184428 (2006).
- ⁵⁶M. V. Indenbom, V. I. Nikitenko, A. A. Polyanskii, and V. V. Vlasko-Vlasov, *Cryogenics* **30**, 747 (1990).
- ⁵⁷L. A. Dorosinskii, M. V. Indenbom, V. I. Nikitenko, Yu. A. Ossip'yan, A. A. Polyanskii, and V. V. Vlasko-Vlasov, *Physica C* **203**, 149 (1992).
- ⁵⁸L. H. Bennett, R. D. McMichael, L. J. Swartzendruber, S. Hua, D. S. Lashmore, A. J. Shapiro, V. S. Gornakov, L. M. Dedukh, and V. I. Nikitenko, *Appl. Phys. Lett.* **66**, 888 (1995).
- ⁵⁹V. I. Nikitenko, L. M. Dedukh, V. S. Gornakov, Yu. P. Kabanov, L. H. Bennett, M. J. Donahue, L. J. Swartzendruber, A. J. Shapiro, and H. J. Brown, *IEEE Trans. Magn.* **33**, 3661 (1997).